

FRACTAL DIMENSION OF COALESCENCE HIDDEN-VARIABLE FRACTAL INTERPOLATION SURFACE

SRIJANANI ANURAG PRASAD* and G. P. KAPOOR†

*Department of Mathematics and Statistics
Indian Institute of Technology Kanpur
Kanpur 208016, India*

**jana@iitk.ac.in*

†gp@iitk.ac.in

Received March 23, 2010
Accepted February 10, 2011

Abstract

In the present paper, the bounds on fractal dimension of Coalescence Hidden-variable Fractal Interpolation Surface (CHFIS) in \mathbb{R}^3 on a equispaced mesh are found. These bounds determine the conditions on the free parameters for fractal dimension of the constructed CHFIS to become close to 3. The results derived here are tested on a tsunami wave surface by computing the lower and upper bounds of the fractal dimension of its CHFIS simulation.

Keywords: Interpolation; IFS; Attractor; Fractal Surface; Fractal Dimension; Tsunami Wave; Hölder Exponent.

1. INTRODUCTION

Among the major recent developments in understanding the structures of objects found in nature, the notion of fractals occupies an important place. Since the introduction of the term *Fractal* by Mandelbrot,¹ an increasing number of research papers have demonstrated the fractal nature of many

systems with different physical properties. Fractal dimension is widely used to quantify the roughness of natural objects and structures. It was demonstrated by Mandelbrot² himself that the notion of fractal dimension is quite useful in quantifying the roughness of irregular patterns such as that of tortuous lines, crumpled surfaces, intricate shapes.

Breslin and Belward³ used fractal dimension to model rainfall time series and discussed suitability of fractal analysis for these type of data. Arakawa and Krotkov⁴ discussed natural terrain modeling using fractal geometry and gave methods of estimation of fractal dimension and fractal surface reconstruction. Lung and Zhang⁵ discussed the origin of the negative correlation between fractal dimension and toughness of fractured surfaces of materials. Zahouani *et al.*⁶ modeled a random surface topography and showed that fractal dimension can be used as an indicator of the real values of different scale-dependent parameters such as length, surfaces and volume of roughness.

Barnsley and Harrington⁷ used shifted composition to express affine Fractal Interpolation Functions (FIFs) and computed their fractal dimensions. Bedford⁸ extended Barnsley's definition of self-affine fractal function to use non-linear scalings and showed that for a class of such functions, the Hölder exponents are related to the box dimension of the function. However, most of the natural objects like surfaces of rocks, sea surfaces, clouds and many naturally occurring structures are made up of both self-affine and non-self-affine parts. In most of the cases, the computation of fractal dimension of these surfaces by existing methods is not practically feasible. The present work is aimed at overcoming this inadequacy by finding the bounds on Fractal Dimension of a Coalescence Hidden Variable Fractal Interpolation Surface (CHFIS), which is generated from a non-diagonal IFS on a equispaced mesh that generates both self-affine and non-self affine FIS simultaneously, depending on free variables and constrained variable.

The organization of the paper is as follows: A brief introduction on construction of CHFIS and its smoothness is given in Sec. 2. Our main results on bounds of Fractal Dimension of CHFIS on equispaced mesh are derived in Sec. 3. Using these bounds, certain conditions on the free parameters are determined that lead the fractal dimension of the constructed CHFIS to become close to 3. Finally, in Sec. 4, to substantiate our results, the bounds on fractal dimension of CHFIS of a Tsunami wave surface are computed.

2. CONSTRUCTION OF CHFIS

Let $\{(x_0, y_0, z_{0,0}), (x_1, y_0, z_{1,0}), \dots, (x_0, y_1, z_{0,1}), \dots, (x_0, y_N, z_{0,1}), \dots, (x_N, y_N, z_{N,N})\}$, $N \in \mathbb{N}$, be an interpolation data in \mathbb{R}^3 such that

$x_0 < x_1 < \dots < x_N$, $y_0 < y_1 < \dots < y_N$ and the independent variables on X and Y axis are equally spaced on a square mesh $[0, \frac{1}{2}] \times [0, \frac{1}{2}]$. For the construction of Coalescence Hidden-variable Fractal Interpolation Surface (CHFIS), a set of real parameters $\{t_{i,j}\}$, called *hidden-variables*, are introduced and the generalized interpolation data $\{(x_i, y_j, z_{i,j}, t_{i,j}) : i, j = 0, 1, \dots, N\}$ is considered. Define the Iterated Function System (IFS)

$$\{\mathbb{R}^4, \omega_{n,m} = (\phi_n(x), \psi_m(y), G_{n,m}(x, y, z, t)) : n, m = 1, 2, \dots, N\}, \tag{2.1}$$

where the functions $\phi_n : [x_0, x_N] \rightarrow [x_{n-1}, x_n]$, $\psi_m : [y_0, y_N] \rightarrow [y_{m-1}, y_m]$ are

$$\begin{aligned} \phi_n(x) &= x_{n-1} + \frac{x_n - x_{n-1}}{x_N - x_0}(x - x_0), \\ \psi_m(y) &= y_{m-1} + \frac{y_m - y_{m-1}}{y_N - y_0}(y - y_0) \end{aligned}$$

and the function $G_{n,m} : [x_0, x_N] \times [y_0, y_N] \times \mathbb{R}^2 \rightarrow \mathbb{R}^2$ is

$$G_{n,m}(x, y, z, t) = \begin{cases} F_{n+1,m}(x_0, y, z, t), & x = x_N, n = 1, \dots, N - 1, \\ & m = 1, \dots, N \\ F_{n,m+1}(x, y_0, z, t), & y = y_N, n = 1, \dots, N, \\ & m = 1, \dots, N - 1 \\ F_{n,m}(x, y, z, t), & \text{otherwise,} \end{cases}$$

with the function $F_{n,m}(x, y, z, t) = (F_{n,m}^1(x, y), F_{n,m}^2(x, y))$ given by

$$\left. \begin{aligned} F_{n,m}^1(x, y, z, t) &= \alpha_{n,m} z + \beta_{n,m} t + e_{n,m} x \\ &\quad + f_{n,m} y + g_{n,m} xy + k_{n,m}, \\ F_{n,m}^2(x, y, t) &= \gamma_{n,m} t + \tilde{e}_{n,m} x + \tilde{f}_{n,m} y \\ &\quad + \tilde{g}_{n,m} xy + \tilde{k}_{n,m}. \end{aligned} \right\} \tag{2.2}$$

In Eq. (2.2), $\alpha_{n,m}$ and $\gamma_{n,m}$ are free variables chosen such that $|\alpha_{n,m}| < 1$ and $|\gamma_{n,m}| < 1$, $\beta_{n,m}$ is a constrained variable chosen such that $|\beta_{n,m}| + |\gamma_{n,m}| < 1$ and the real coefficients $e_{n,m}$, $f_{n,m}$, $g_{n,m}$, $k_{n,m}$, $\tilde{e}_{n,m}$, $\tilde{f}_{n,m}$, $\tilde{g}_{n,m}$ and $\tilde{k}_{n,m}$ are obtained by the join-up conditions:

$$\left. \begin{aligned} F_{n,m}(x_0, y_0, z_{0,0}, t_{0,0}) &= (z_{n-1,m-1}, t_{n-1,m-1}) \\ F_{n,m}(x_N, y_0, z_{N,0}, t_{N,0}) &= (z_{n,m-1}, t_{n,m-1}) \\ F_{n,m}(x_0, y_M, z_{0,M}, t_{0,M}) &= (z_{n-1,m}, t_{n-1,m}) \\ F_{n,m}(x_N, y_M, z_{N,M}, t_{N,M}) &= (z_{n,m}, t_{n,m}). \end{aligned} \right\} \tag{2.3}$$

It is known⁹ that there exists a metric τ on \mathbb{R}^4 , equivalent to the Euclidean metric, such that the IFS, given by Eq. (2.1), is hyperbolic with respect to the metric τ and there exists a unique non-empty compact set $G \subseteq \mathbb{R}^4$ with respect to the metric τ such that $G = \cup_{n=1}^N \cup_{m=1}^N \omega_{n,m}(G)$. The set G , called the *attractor* of the IFS for the given interpolation data, is the graph of a continuous function $F: [x_0, x_N] \times [y_0, y_N] \rightarrow \mathbb{R}^2$ such that $F(x_i, y_j) = (z_{i,j}, t_{i,j})$ for $i, j = 0, 1, \dots, N$, i.e. $G = \{(x, y, F(x, y)) : (x, y) \in [x_0, x_N] \times [y_0, y_N] \text{ and } F(x, y) = (z(x, y), t(x, y))\}$. Now, expressing the function $F(x, y)$ component-wise as $F(x, y) = (F_1(x, y), F_2(x, y))$, the Coalescence Hidden-variable Fractal Interpolation Surface (CHFIS) for the given interpolation data is defined as follows:

Definition 2.1. The **Coalescence Hidden-variable Fractal Interpolation Surface (CHFIS)** for the given interpolation data $\{(x_i, y_j, z_{i,j}) : i, j = 0, 1, \dots, N\}$ is defined as the function $F_1(x, y)$ whose graph is the projection of the graph of the function $F(x, y)$ on \mathbb{R}^3 .

A set S of points $x = (x_1, x_2, \dots, x_n)$ in a Euclidean space of dimension n is called *self-affine* if S is union of N distinct subsets, each identical with $aS = \{(a_1x_1, a_2x_2, \dots, a_nx_n) : a = (a_1, a_2, \dots, a_n), a_i > 0 \text{ and } x \in S\}$ up to translation and rotation. If S is not self-affine, then it is called *non-self-affine*. The function $F_1(x, y)$ occurring in Definition 2.1 is called a CHFIS as it exhibits both self-affine and non-self-affine nature. We observe that the function $F_2(x, y)$ for the same interpolation data is always a self-affine function.

Fractal Dimension of a CHFIS $F_1(x, y)$ is the box counting dimension¹⁰ of its graph defined as

$$D(\text{Graph}(F_1(x, y))) = \lim_{n \rightarrow \infty} \frac{\log(\mathcal{N}_n(\text{Graph}(F_1(x, y))))}{\log 2^n};$$

provided the limit exist, $\mathcal{N}_n(\text{Graph}(F_1(x, y)))$ being the smallest number of closed boxes in \mathbb{R}^3 of side $\frac{1}{2^n}$ that intersect the graph of CHFIS $F_1(x, y)$.

A function $F: \mathbb{R}^2 \rightarrow \mathbb{R}$ is said to be a *Lip-schitz function of order δ* (written as $\text{Lip } \delta$) if $|F(X) - F(\bar{X})| \leq K (d_M(X, \bar{X}))^\delta$ where, K is a constant, $\delta \in (0, 1]$ and $d_M(X, \bar{X}) = |x - \bar{x}| + |y - \bar{y}|$ for $X = (x, y)$, $\bar{X} = (\bar{x}, \bar{y})$. The function F is said to be a $\text{Lip}_k^* \delta$ function, if $|F(X) - F(\bar{X})| \leq \bar{K} [(d_M(X, \bar{X}))^\delta [1 + \log(d_M(X, \bar{X}))^k]]$, where \bar{K} is a

constant, $\delta \in (0, 1]$ and $k \in \mathbb{N}$. Denote,

$$\left. \begin{aligned} p_{n,m}(x, y) &= e_{n,m} x + f_{n,m} y + g_{n,m} xy + k_{n,m} \\ q_{n,m}(x, y) &= \tilde{e}_{n,m} x + \tilde{f}_{n,m} y + \tilde{g}_{n,m} xy + \tilde{k}_{n,m}. \end{aligned} \right\} \quad (2.4)$$

It is observed that the functions $p_{n,m}(x, y)$ and $q_{n,m}(x, y)$, given by Eq. (2.4), belong to the classes $\text{Lip } \lambda_{n,m}$ and $\text{Lip } \mu_{n,m}$ ($0 < \lambda_{n,m}, \mu_{n,m} \leq 1$) respectively.

The following notations are used in the sequel.

Notations. $I = [x_0, x_N]$; $J = [y_0, y_N]$; $I_n = [x_{n-1}, x_n]$; $J_m = [y_{m-1}, y_m]$; $I_{\min} = \min\{|I_n| : n = 1, \dots, N\}$; $I_{\max} = \max\{|I_n| : n = 1, \dots, N\}$; $J_{\min} = \min\{|J_m| : m = 1, \dots, N\}$; $J_{\max} = \max\{|J_m| : m = 1, \dots, N\}$; $S_{n,m} = I_n \times J_m$; $S_{\min} = I_{\min} \times J_{\min}$; $S_{\max} = I_{\max} \times J_{\max}$; $\lambda = \min\{|\lambda_{n,m}| : n, m = 1, \dots, N\}$; $\mu = \min\{|\mu_{n,m}| : n, m = 1, \dots, N\}$; $\Omega_{n,m} := \frac{\alpha_{n,m}}{|S_{n,m}|^\lambda}$; $\Gamma_{n,m} := \frac{\gamma_{n,m}}{|S_{n,m}|^\mu}$; $\Theta_{n,m} := \frac{\alpha_{n,m}}{|S_{n,m}|^\mu}$. Further, we denote

$$\left. \begin{aligned} \Omega &= \max\{|\Omega_{n,m}| : n, m = 1, 2, \dots, N\} \\ \Gamma &= \max\{|\Gamma_{n,m}| : n, m = 1, 2, \dots, N\} \\ \Theta &= \max\{|\Theta_{n,m}| : n, m = 1, 2, \dots, N\}. \end{aligned} \right\} \quad (2.5)$$

Definition 2.2. The Bivariate CHFIS $F_1(x, y)$ is called a **Critical CHFIS** if any one of the conditions $\Omega = 1$, $\Gamma = 1$ and $\Theta = 1$ holds.

3. FRACTAL DIMENSION OF CHFIS

In this section, the bounds on the fractal dimension of CHFIS $F_1(x, y)$ for different critical cases are obtained in Theorems 3.1 and 3.2. Using these bounds, certain conditions on the free parameters are determined that lead the fractal dimension of the constructed CHFIS to become close to 3. Also, these bounds give us a range of the free parameters that ensure the fractal dimension of the constructed CHFIS to be strictly greater than 2. Let $I_{r_1, \dots, r_n} \equiv \phi_{r_n}(0) + |I_{r_n}| I_{r_1, \dots, r_{n-1}} = \phi_{r_n} \circ \dots \circ \phi_{r_1}(I)$ and $J_{s_1, \dots, s_n} \equiv \psi_{s_n}(0) + |J_{s_n}| J_{s_1, \dots, s_{n-1}} = \psi_{s_n} \circ \dots \circ \psi_{s_1}(J)$, $r_i, s_j \in \{1, 2, \dots, N\}$, where $|I_{r_i}|$ and $|J_{s_j}|$ denote the length of the intervals I_{r_i} and J_{s_j} respectively. Hence, the area of square $S_{r_1, \dots, r_n, s_1, \dots, s_n} = I_{r_1, \dots, r_n} \times J_{s_1, \dots, s_n}$ is $|S_{r_1, \dots, r_n, s_1, \dots, s_n}| = |I_{r_1, \dots, r_n}| \times |J_{s_1, \dots, s_n}| = |I_{r_1}| \times |J_{s_1}| \times \dots \times |I_{r_n}| \times |J_{s_n}| = |S_{r_1, s_1}| \times \dots \times |S_{r_n, s_n}|$ and the diameter $\text{diam}_M(S_{r_1, \dots, r_n, s_1, \dots, s_n})$ of the square $S_{r_1, \dots, r_n, s_1, \dots, s_n}$ is $|I_{r_1, \dots, r_n}| + |J_{s_1, \dots, s_n}|$.

The following theorem give the bounds on the fractal dimension of CHFIS $F_1(x, y)$ when $\Theta \neq 1$ and $\Omega = 1$ or $\Gamma = 1$.

Theorem 3.1. *Let $F_1(x, y)$ be a CHFIS with $\Theta \neq 1$. Then, for the critical condition $\Omega = 1$,*

$$\zeta(\alpha_{i,j}) \leq D(\text{Graph}(F_1(x, y))) \leq 3 - \delta(\Gamma) \quad (3.1)$$

where $\zeta(\alpha_{i,j}) = \max\{1 + \frac{\log(\sum_{i=1}^N \sum_{j=1}^N |\alpha_{i,j}|)}{\log N}, 2\}$ and $\delta(\Gamma) \in (0, 1]$. Further, for the critical condition $\Gamma = 1$,

$$\eta(\gamma_{i,j}) \leq D(\text{Graph}(F_1(x, y))) \leq 3 - \delta(\Omega), \quad (3.2)$$

where $\eta(\gamma_{i,j}) = \max\{1 + \frac{\log(\sum_{i=1}^N \sum_{j=1}^N |\gamma_{i,j}|)}{\log N}, 2\}$ and $\delta(\Omega) \in (0, 1]$.

Proof. Case (i): ($\Theta \neq 1, \Omega = 1$ and $\Gamma \neq 1$) In this case, there exist constants C_1 and C_2 such that¹¹

$$\begin{aligned} C_1(d_M(X, \bar{X}))^{\delta(\Gamma)} &\leq d_M(F_1(X), F_1(\bar{X})) \\ &\leq C_2(d_M(X, \bar{X}))^{\delta(\Gamma)} \\ &\quad \times [1 + \log(d_M(X, \bar{X}))], \end{aligned} \quad (3.3)$$

for some $\delta(\Gamma) \in (0, 1]$, $X = (x, y)$, $\bar{X} = (\bar{x}, \bar{y})$, $0 \leq x < \bar{x} \leq \frac{1}{2}$ and $0 \leq y < \bar{y} \leq \frac{1}{2}$. In fact, $\delta(\Gamma) = \min(\lambda, \mu)$ or $\min(\lambda, \tau_1)$ if $\Gamma \leq 1$ and $\delta(\Gamma) = \min(\lambda, \tau_2)$ or $\delta = \min(\lambda, \tau_3)$ if $\Gamma > 1$ where, τ_1, τ_2 and τ_3 are non-negative real numbers in the interval $(0, 1]$ such that $\tau_1 \leq \frac{\log \alpha}{\log |S_{\min}|}$, $\tau_2 \leq \frac{\log \gamma}{\log |S_{\min}|}$ and $\tau_3 \leq \frac{\log(\alpha\gamma)}{\log |S_{\min}|} - \mu$.

Let $G_{r_1, \dots, r_m, s_1, \dots, s_m} = \{(X, F_1(X), F_2(X)) : X \in S_{r_1, \dots, r_m, s_1, \dots, s_m}\}$. Then, $\max\{d_M(X, \bar{X}) : X, \bar{X} \in S_{r_1, \dots, r_m, s_1, \dots, s_m}\} = \text{diam}_M(S_{r_1, \dots, r_m, s_1, \dots, s_m})$ and $|G_{r_1, r_2, \dots, r_m, s_1, s_2, \dots, s_m}| \equiv \max\{d_M(F_1(X), F_1(\bar{X})) : (X, \bar{X}) \in S_{r_1, \dots, r_m, s_1, \dots, s_m}\}$. Then, by Eq. (3.3),

$$\begin{aligned} C_1[\text{diam}_M(S_{r_1, \dots, r_m, s_1, \dots, s_m})]^{\delta(\Gamma)} &\leq |G_{r_1, \dots, r_m, s_1, \dots, s_m}| \\ &\leq C_2[\text{diam}_M(S_{r_1, \dots, r_m, s_1, \dots, s_m})]^{\delta(\Gamma)} \\ &\quad \times [1 + \log(\text{diam}_M(S_{r_1, \dots, r_m, s_1, \dots, s_m}))]. \end{aligned} \quad (3.4)$$

Choose m large such that $[\text{diam}_M(S_{\max})]^m < \frac{1}{2^n}$ for $n \in \mathbb{N}$. Now, $\Omega_{r_i, s_j} \leq \Omega = 1$ implies $|\alpha_{r_i, s_j}| \leq (|S_{r_i, s_j}|)^\lambda \leq (|S_{r_i, s_j}|)^{\delta(\Gamma)}$. Hence, $\prod_{i=1}^m |\alpha_{r_i, s_i}| \leq \prod_{i=1}^m |S_{r_i, s_i}|^{\delta(\Gamma)} = |S_{r_1, r_2, \dots, r_m, s_1, s_2, \dots, s_m}|^{\delta(\Gamma)} \leq [\text{diam}_M(S_{r_1, r_2, \dots, r_m, s_1, s_2, \dots, s_m})]^{\delta(\Gamma)}$. Further, since $\text{diam}_M(S_{r_i, s_j}) = \frac{1}{N}$ for all i and j , $[\text{diam}_M$

$(S_{r_1, r_2, \dots, r_m, s_1, s_2, \dots, s_m})] \leq [\text{diam}_M(S_{r_i, s_j})]^m = (\frac{1}{N})^m$ for any i and j . Therefore, it follows from (3.4)

$$\begin{aligned} C_1 \prod_{i=1}^m |\alpha_{r_i, s_i}| &\leq |G_{r_1, r_2, \dots, r_m, s_1, s_2, \dots, s_m}| \\ &\leq C_2 \left(\frac{1}{N}\right)^{m\delta(\Gamma)} \left[1 + \log\left(\frac{1}{N}\right)^m\right]. \end{aligned}$$

Taking summation over r_1, r_2, \dots, r_m and s_1, s_2, \dots, s_m from 1 to N we have

$$\begin{aligned} C_1 N^m \sum_{r_1, \dots, r_m} \sum_{s_1, \dots, s_m} \prod_{i=1}^m |\alpha_{r_i, s_i}| &\leq N^m \sum_{r_1, \dots, r_m} \sum_{s_1, \dots, s_m} |G_{r_1, \dots, r_m, s_1, \dots, s_m}| \\ &\leq \left\{ C_2 \left(\frac{1}{N}\right)^{m(\delta(\Gamma)-1)} \left[1 + \log\left(\frac{1}{N}\right)^m\right] \right\} \\ &\quad \times \sum_{r_1, \dots, r_m} \sum_{s_1, \dots, s_m} 1. \end{aligned}$$

The above inequality implies

$$\begin{aligned} C_1 N^m \left[\sum_{i=1}^N \sum_{j=1}^N (|\alpha_{i,j}|) \right]^m &\leq \mathcal{N}_n(\text{Graph}(F_1(x, y))) \\ &\leq \left\{ C_2 \left(\frac{1}{N}\right)^{m(\delta(\Gamma)-1)} \left[1 + \log\left(\frac{1}{N}\right)^m\right] \right\} \cdot N^{2m}. \end{aligned}$$

The bound on fractal dimension of CHFIS $F_1(x, y)$ given by Eq. (3.1) follow from the above inequalities and $\zeta(\alpha_{i,j}) = \max\{1 + \frac{\log(\sum_{i=1}^N \sum_{j=1}^N |\alpha_{i,j}|)}{\log N}, 2\}$.

Case (ii): ($\Theta \neq 1, \Gamma = 1$ and $\Omega \neq 1$) The proof is similar to case (i) up to Eq. (3.4). In the present case, since $\Gamma = 1$, $\gamma_{r_i, s_j} \leq (|S_{r_i, s_j}|)^\mu \leq (|S_{r_i, s_j}|)^{\delta(\Omega)}$, where, $\delta(\Omega) \in (0, 1]$ is given by $\delta(\Omega) = \min(\lambda, \mu)$ or $\min(\lambda, \tau_1)$ for $\Omega \leq 1$ and $\delta(\Omega) = \tau_1$ for $\Omega > 1$.¹¹ Hence,

$$\begin{aligned} \prod_{i=1}^m |\gamma_{r_i, s_i}| &\leq \prod_{i=1}^m |S_{r_i, s_i}|^{\delta(\Omega)} \\ &= |S_{r_1, r_2, \dots, r_m, s_1, s_2, \dots, s_m}|^{\delta(\Omega)} \leq \left(\frac{1}{N}\right)^{m\delta(\Omega)}. \end{aligned}$$

Therefore, it follows from (3.4),

$$C_1 \prod_{i=1}^m |\gamma_{r_i, s_i}| \leq |G_{r_1, r_2, \dots, r_m, s_1, s_2, \dots, s_m}| \leq C_2 \left(\frac{1}{N}\right)^{m\delta(\Omega)} \left[1 + \log\left(\frac{1}{N}\right)^m\right].$$

Taking summation over r_1, r_2, \dots, r_m and s_1, s_2, \dots, s_m from 1 to N , we have

$$C_1 N^m \sum_{r_1, \dots, r_m} \sum_{s_1, \dots, s_m} \prod_{i=1}^m |\gamma_{r_i, s_i}| \leq N^m \sum_{r_1, \dots, r_m} \sum_{s_1, \dots, s_m} |G_{r_1, \dots, r_m, s_1, \dots, s_m}| \leq \left\{ C_2 \left(\frac{1}{N}\right)^{m(\delta(\Omega)-1)} \left[1 + \log\left(\frac{1}{N}\right)^m\right] \right\} \times \sum_{r_1, \dots, r_m} \sum_{s_1, \dots, s_m} 1.$$

The above inequality implies

$$C_1 N^m \left[\sum_{i=1}^N \sum_{j=1}^N (|\gamma_{i,j}|) \right]^m \leq \mathcal{N}_n(\text{Graph}(F_1(X))) \leq \left\{ C_2 \left(\frac{1}{N}\right)^{m(\delta(\Omega)-1)} \left[1 + \log\left(\frac{1}{N}\right)^m\right] \right\} \cdot N^{2m}.$$

The bound on fractal dimension of CHFIS $F_1(x, y)$ given by Eq. (3.2) follow from the above inequalities and $\eta(\gamma_{i,j}) = \max\{1 + \frac{\log(\sum_{i=1}^N \sum_{j=1}^N |\gamma_{i,j}|)}{\log N}, 2\}$. □

Theorem 3.2 give us the bounds on the fractal dimension of CHFIS $F_1(x, y)$ when $\Theta = 1$.

Theorem 3.2. Let $F_1(x, y)$ be a CHFIS with $\Theta = 1$. Then,

$$\zeta(\alpha_{i,j}) \leq D_F(\text{Graph}(F_1(x, y))) \leq 3 - \delta(\Omega, \Gamma), \tag{3.5}$$

where $\zeta(\alpha_{i,j}) = \max\{1 + \frac{\log(\sum_{i=1}^N \sum_{j=1}^N |\alpha_{i,j}|)}{\log N}, 1\}$ and $\delta(\Omega, \Gamma) \in (0, 1]$.

Proof. Since $\Theta = 1$, $\Theta_{r_i, s_j} \leq \Theta = 1$ implies $|\alpha_{r_i, s_j}| \leq (|S_{r_i, s_j}|)^\mu \leq (|S_{r_i, s_j}|)^{\delta(\Omega, \Gamma)}$, where,

- (i) $\delta(\Omega, \Gamma) = \min(\lambda, \mu)$ for $\Omega \leq 1, \Gamma \leq 1$,
- (ii) $\delta(\Omega, \Gamma) = \min(\tau_1, \mu)$ for $\Omega > 1, \Gamma \leq 1$,
- (iii) $\delta(\Omega, \Gamma) = \min(\lambda, \tau_2)$ for $\Omega \leq 1, \Gamma > 1$ and
- (iv) $\delta(\Omega, \Gamma) = \min(\tau_1, \tau_2)$ for $\Omega > 1, \Gamma > 1$.¹¹

The rest of the proof is similar to the proof of Theorem 3.1 and hence is omitted. □

Remark 3.1. Using Theorems 3.1 and 3.2, it follows that the constructed CHFIS has fractal dimension close to 3 if (i) $|\alpha_{i,j}|$ is sufficiently close to 1 and $\Omega = 1$ or $\Theta = 1$ or, (ii) $|\gamma_{i,j}|$ is sufficiently close to 1 and $\Gamma = 1$. For, if $\Omega = 1$ or $\Theta = 1$ or $\Gamma = 1$, then λ or μ is sufficiently close to 0 so that $\delta(\Gamma), \delta(\Omega)$ or $\delta(\Omega, \Gamma)$ is also sufficiently close to 0 since these values are bounded by λ or μ .

Remark 3.2. It follows from Theorems 3.1 and 3.2 that

$$2 < D(\text{Graph}(F_1(x, y))) < 3 \tag{3.6}$$

if (i) $(\frac{1}{N}) < |\alpha_{i,j}| \leq (\frac{1}{2N})^{2p}$ where $p = \lambda$ for $\Omega = 1$ and $p = \mu$ for $\Theta = 1$ or (ii) $(\frac{1}{N}) < |\gamma_{i,j}| \leq (\frac{1}{2N})^{2\mu}$ and $\Gamma = 1$.

4. EXAMPLE

Consider the sample data given by Table 1 taken from a tsunami wave surface (Fig. 1) and the generalized interpolation data given by Table 2.

Table 3 gives choices of parameters $\alpha_{n,m}, \gamma_{n,m}$ and $\beta_{n,m}$ corresponding to critical conditions $\Theta = 1$,

Table 1 Surface Values $z_{n,m}$ at (x_n, y_m) in Interpolation Data.

y_m/x_n	0	0.0998	0.1996	0.2994	0.3992	0.499
0	0.23	0.2	0.2	0.2	0.31	0.18
0.0998	0.36	0.26	0.23	0.24	0.24	0.23
0.1996	0.26	0.26	0.37	0.26	0.26	0.25
0.2994	0.32	0.29	0.27	0.3	0.36	0.3
0.3992	0.21	0.24	0.26	0.29	0.29	0.3
0.499	0.26	0.26	0.29	0.28	0.28	0.29

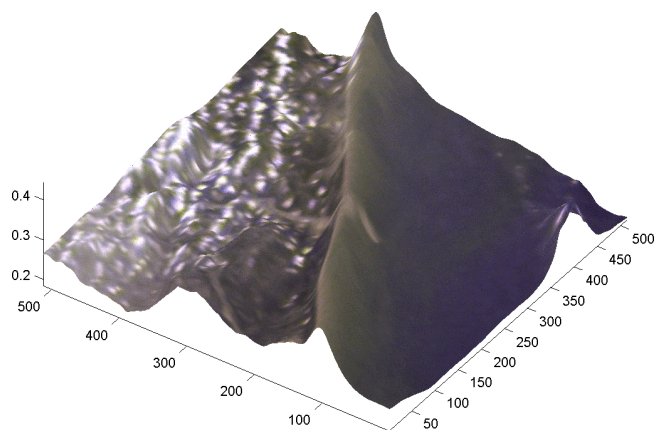


Fig. 1 Tsunami wave surface in three-dimensional view.

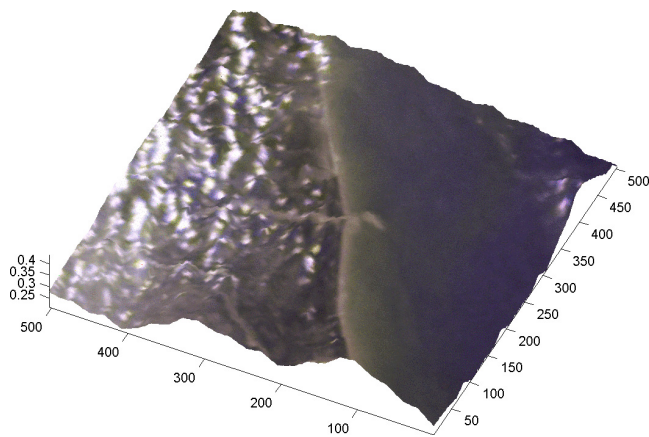
Table 2 Sample Values $t_{n,m}$ at (x_n, y_m) in Generalized Interpolation Data.

y_m/x_n	0	0.0998	0.1996	0.2994	0.3992	0.499
0	0.2	0.6	0.62	0.37	0.57	0.45
0.0998	0.04	0.02	0.31	0.01	0.38	0.68
0.1996	0.09	0.03	0.61	0.6	0.01	0.01
0.2994	0.19	0.58	0.05	0.36	0.63	0.71
0.3992	0.69	0.08	0.45	0.44	0.35	0.15
0.499	0.67	0.69	0.72	0.47	0.55	0.12

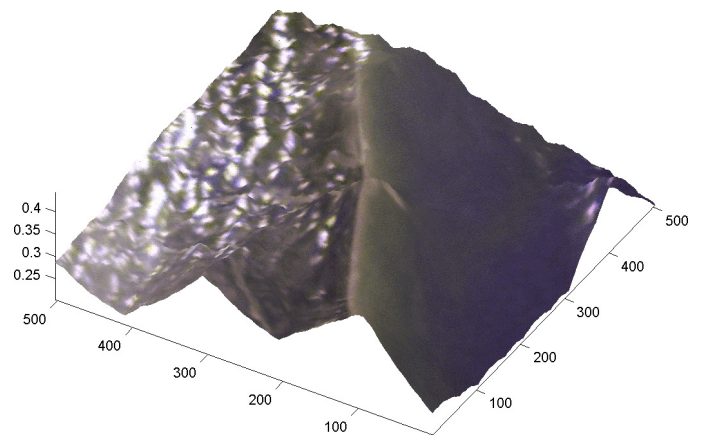
$\Omega = 1$ or $\Gamma = 1$ for the simulation of the tsunami wave surface as a CHFIS. The values of these parameters are determined by requiring that the functions $p_{n,m}$ and $q_{n,m}$ defined by Eq. (2.4) are in suitable classes $\text{Lip } \lambda_{n,m}$ and $\text{Lip } \mu_{n,m}$ respectively such that the value of Θ , Ω or Γ (c.f. Eq. (2.5)) equals 1. The last three columns in Table 3 give corresponding δ -value of simulated CHFIS, lower bound and upper bound (c.f. Inequalities (3.1), (3.2) and (3.5)) of its fractal dimension. Figures 2(a)–2(c) give the simulations

Table 3 Choices of Free Parameters $\alpha_{n,m}, \gamma_{n,m}, \beta_{n,m}$, Computed Values of $\Theta, \Omega, \Gamma, \delta$ and Bounds on Fractal Dimension of CHFIS (c.f. Figs. 2(a)–2(c)).

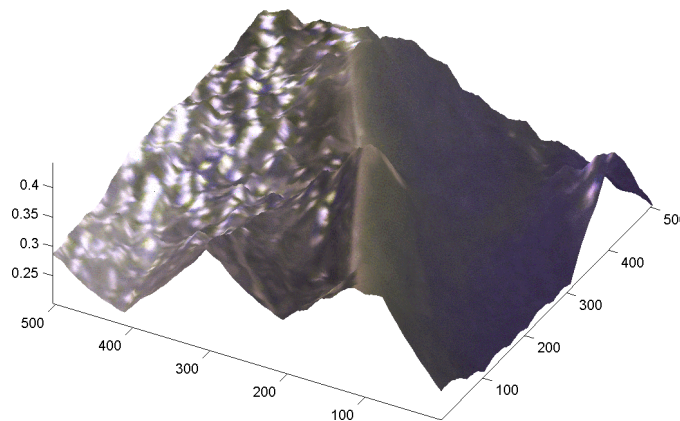
Fig.	$\alpha_{n,m}$	$\gamma_{n,m}$	$\beta_{n,m}$	Θ	Ω	Γ	δ	Lower Bound on Fractal Dimension	Upper Bound on Fractal Dimension
2(a)	0.22	0.3	0.02	1	21.99	1.18	0.2614	2.0592	2.7386
2(b)	0.0101	0.2	0.02	0.05	1	1.16	0.3492	2	2.6508
2(c)	0.22	0.1348	0.02	1.64	21.99	1	0.3285	2	2.6715



(a) CHFIS simulation for Critical Case $\Theta = 1$.



(b) CHFIS simulation for Critical Case $\Omega = 1$.



(c) CHFIS simulation for Critical Case $\Gamma = 1$.

Fig. 2 CHFIS simulation of tsunami wave surface.

of the tsunami wave surface (c.f. Fig. 1) as CHFIS under different critical conditions corresponding to the choices of free parameters in Table 3.

It is observed in Table 3 that the critical condition $\Theta = 1$ gives the largest lower bound on the fractal dimension of the corresponding CHFIS (c.f. Fig. 2(a)) while the critical condition $\Omega = 1$ gives the least upper bound on the fractal dimension of the corresponding CHFIS (c.f. Fig. 2(b)). In case of the critical condition $\Gamma = 1$, the upper and lower bounds on the fractal dimension of the corresponding CHFIS (c.f. Fig. 2(c)) are not the least and largest bounds respectively. Thus, for the above Tsunami wave surface (c.f. Fig. 1) and the generalized interpolation data (c.f. Table 2), the critical condition $\Theta = 1$ or $\omega = 1$ give closer bounds (lower or upper respectively) on the fractal dimension of its simulated CHFIS.

The box counting dimension of the Tsunami wave surface (c.f. Fig. 1) in our present example has also been computed and found to be 2.1377, substantiating the inequalities (3.1), (3.2) and (3.5).

5. CONCLUSIONS

In this paper, the bounds on Fractal Dimension of Coalescence Hidden-variable Fractal Interpolation Surface (CHFIS) are determined. Using these bounds on Fractal Dimension of CHFIS, certain conditions on the free parameters are found that lead the fractal dimension of the constructed CHFIS to become close to 3. As a test case, a tsunami wave surface is considered and the bounds, found in the present work, on fractal dimension of its simulated CHFIS are computed to substantiate our results. Besides other applications in diverse fields of science and engineering (viz. Refs. 12–14), the bounds on fractal dimensions of CHFIS found here are likely to be helpful in the development of models for computation of tsunami intensity.

ACKNOWLEDGMENTS

The author Srijanani thanks CSIR for research grant (No:9/92(417)/2005-EMR-I) for the present work.

REFERENCES

1. B. B. Mandelbrot, Stochastic models of the earth's relief, the shape and the fractal dimension of the coastlines and the number-area rule for islands, *Proc. Natl. Acad. Sci. USA* **72** (1975) 3825–3828.
2. B. B. Mandelbrot, *The Fractal Geometry of Nature* (W. H. Freeman and Co., New York, 1982).
3. M. C. Breslin and J. A. Belward, Fractal dimensions for rainfall time series, *Math. Comput. Simul.* **48** (1999) 437–446.
4. K. Arakawa and E. Krotkov, Fractal modelling of natural terrain: analysis and surface reconstruction with range data, *Graph. Model Image Process* **58**(5) (1996) 413–436.
5. C. W. Lung and S. Z. Zhang, Fractal dimension of the fractured surface of materials, *Physica* **38** (1989) 242–245.
6. H. Zahouani, R. Vargiolu and J. L. Loubet, Fractal models of surface topography and contact mechanics, *Math. Comput. Model.* **28**(4) (1998) 517–534.
7. M. F. Barnsley and A. N. Harrington, The calculus of fractal interpolation functions, *J. Approx. Theory* **57** (1989) 14–34.
8. T. Bedford, Holder exponents and box dimension for self affine fractal functions, *Constr. Approx.* **5** (1989) 33–48.
9. A. K. B. Chand and G. P. Kapoor, Hidden variable bivariate fractal interpolation surfaces, *Fractals* **11**(3) (2003) 227–288.
10. M. F. Barnsley, *Fractals Everywhere* (Academic Press, Orlando, Florida, 1988).
11. G. P. Kapoor and S. A. Prasad, Smoothness of hidden variable bivariate coalescence fractal interpolation surfaces, *Int. J. Bifurc. Chaos* **19**(7) (2009) 2321–2333.
12. U. R. Acharya, P. S. Bhat, N. Kannathal, A. Rao and C. M. Lim, Analysis of cardiac health using fractal dimension and wavelet transformation, *ITBM RBM* **26** (2005) 133–139.
13. J. G. Jones, R. W. Thomas and P. G. Earwicker, Fractal properties of computer-generated and natural geophysical data, *Comput. Geosci.* **15**(2) (1989) 227–235.
14. S. E. G. Mayer-Kress, Observations of the fractal dimensions of deep and shallow water ocean surface gravity waves, *Physica* **37** (1989) 104–108.